Robert Czech, Marek Mróz, Janusz Pikuła, Marcin Spólnik, Bogdan Kupiec, Andrzej Dec, Marek Węglowski

DOI: 10.32730/mswt.2023.67.5-6.6

Numerical Simulation and the Improved Welding of Storage Tank Heads with Respect to Minimised Welding Strains

Abstract: The article presents results of Sysweld software programme-based tests involving the use of numerical simulation in the improvement of the welding of a storage tank head with respect to the minimisation of welding strains (distortions). The development of CAD models and mock-ups used in the FEM analysis was based on drawing documentation. The numerical simulation concerning the distribution of the field of displacements in the storage tank head was performed for four models, involving various welding sequences and directions. Related analyses involved the initial model applied in the technology currently used in the fabrication of storage tank heads as well as three new models (of welding sequences and directions). The comparative analysis, involving the initial model and the three new models, was concerned with different values of displacements in all directions (X, Y and Z) and at all characteristic points of the storage tank head. The simulation results revealed the existence of correlations between welding sequence and directions and varied distributions of fields of displacements (strains/distortions). Post-weld distributions of fields of displacements in the initial model and models 2-4 were characterised by varied values of displacements, yet also by the similar nature of tank head stress-triggered distortions. Dimensionally relevant displacements (distortions) of the storage tank head were observed in direction Z (i.e. direction perpendicular to the surface). In all the models subjected to analysis, the greatest displacements were identified in the areas of storage tank head nodes. Selected welding stages in the initial model were characterised by greater displacements than those observed in models 2-4. In line 1, higher values were observed at stages 8-10, 12 and 13. In turn, in line 2, higher values were observed at stages 8-10. In addition, in line 2, stages 11-14 were characterised by greater displacements in the initial model if compared with those identified in models 3 and 4. The FEM-based analysis of the tank head enabled the qualitative verification of tank-related welding schemes in terms of welding strains.

Key words: MAG, numerical simulation, storage tank, large-size structure, welding strains

1. Introduction

Welding stresses and strains are some of the more important issues accompanying the fabrication of welded structures, particularly large-sized ones and characterised by complicated shapes.

A common feature of all welding methods is the use of a heat source aimed to melt the filler metal and form a liquid metal pool, which, after fast cooling, will form a weld. The heat source affects also the remaining areas of the welded joints, in particular the nearby areas of the base material of elements subjected to welding. Usually, such a situation leads to unfavourable changes including the formation of the hard and brittle heat affected zone (HAZ) or welding strains, which after exceeding a critical value, may trigger the formation of cracks. Factors accompanying the welding thermal cycle, such as fast heating and cooling, changes of values of mechanical parameters as well as phase transformations in the heat affected zone (HAZ) contribute to the mechanical interaction of adjacent elements of the welded structure. Significantly varying temperatures of the above-named areas lead to the formation of stresses inducing the formation of welding strains [1].

Importantly, welding strains can be present along every direction. For instance, strains in longitudinal and transverse directions lead to the formation of the so-called twists. Designers of welded structures and welding engineers have numerous tools and methods making it possible to reduce the presence of welding strains or minimise their adverse effect on welded joins. The aforesaid tools and methods are, among other things, the following [1]:

- design of structures containing a minimum number of welded joints (welds),
- reduction of cross-sections and lengths of welds,
- use of intermittent (skip) welds,
- use of two-sided butt welds,
- avoidance of the crossing of welds,
- appropriate methodology applied when preparing elements to be joined,
- use of appropriate welding methods and beading techniques,
- use of backing strips or other elements aimed at the forced cooling of a joint being welded,

mgr inż. Robert Czech, inż. Marcin Spólnik – Naftoremont-Naftobudowa Sp. z o.o.

dr hab. inż. Marek Mróz, dr inż. Bogdan Kupiec, mgr inż. Andrzej Dec – Politechnika Rzeszowska, Katedra Odlewnictwa i Spawalnictwa / Rzeszow University of Technology

dr inż. Janusz Pikuła, dr inż. Marek Węglowski – Sieć Badawcza Łukasiewicz – Górnośląski Instytut Technologiczny, Centrum Spawalnictwa / ukasiewicz Research Network – Upper Silesian Institute of Technology

Corresponding Author: robert.czech@naftoremont.pl

- use of counterstrain,
- mechanical stress relief (initial stiffening).

When designing welded structures it is necessary to strive after the minimum number of welds, e.g. by using hot-rolled or cold-bent sections (angle sections, T-bars, U-bars etc.) as components. The excessively high energy of the entire welding process, resulting from a large number of welds, can be decreased by reducing the length and cross-sections of welds, without compromising the obtainment of appropriate mechanical properties of welded joints. The length of welds can be limited by means of rolled sections. A decrease in weld cross-section (in some justified cases) can be obtained by using incomplete butt welds. Favourable results arising from the reduced welding thermal cycle effect can be achieved by making intermittent welds. However, it should be noted that such a solution cannot be applied in welded structures exposed to variable loads or to an aggressive corrosive environment. The "replacement" of the one-sided weld with the two-sided one favours the reduction of welding strains and is related to the effect of appropriate welding sequence. The appropriate division of a given structure into individual elements (subsequently joined/welded) is another method enabling the reduction of welding strains. The above-named solution should be applied by design engineers at the design stage and, afterwards, analysed by welding engineers and technologists. It is particularly important to avoid the crossing of welds. The beading technique also significantly affects the level of welding strains. Stepped segmental backward welding significantly reduces welding deformations. Another frequently used method enabling the minimisation of welding strains involves the application of the so-called counterstrain. The appropriate adjustment of counterstrain value enables the making of welded structures of required shape and dimensions. In cases of large and complicated welded structures, the fabrication of which is characterised by the variety of short and long welding thermal cycles, a good method enabling the minimisation welding strains consists in the use of mechanical stress relief. The reduction of (internal) welding stresses is obtained by imposing an appropriate external load to the welded structure. The achievement of the aforesaid result requires the satisfaction of a condition, where the sum of stresses derived from external load(s) and internal stresses must equal the yield point of a material subjected to welding [1, 2].

Welding strains depend primarily on the cross-section of the weld, rigidity, the size of the structure and a heat input, directly connected with a given welding method. The reduction of a heat input translates into a smaller liquid metal pool, which, in turn, leads to smaller thermal shrinkage and, consequently, the reduction of stresses and/or strains. The use of appropriate methods (such as CMT, ColdArc, STT, CBT and HLAW [2]) enables the reduction of internal stresses in welded elements. Notably beneficial in this respect can also be the use of pulsed current of variable polarity in low-energy welding methods such as AC Pulse, Cold Process and CMT Advanced [3–6].

The total elimination of post-weld stresses is difficult, if not impossible. However, it is necessary to try and reduce their effect on the quality of welded structures. Welding engineers can use many solutions enabling the achievement of the aforesaid goal and including both thermal and mechanical methods. The minimisation of the effect of factors triggering the formation of welding strains can also be achieved through the appropriate selection of welding process parameters. Yet, such activities usually entail increased investments and extended production time [7, 8].

The development of computer-aided simulation techniques enabled the increasingly frequent application of welding processes simulation aimed to optimise and improve the fabrication of welded structures. The use of cutting-edge software programmes for the numerical simulation of phenomena and processes present during the welding process makes it possible to shorten the time necessary for the development of technologies used in the fabrication of welded structures and reduce fabrication-related expenses [9, 10].

Numerical simulations are used in relation to such welding methods as MIG [7, 11, 12–15], MAG [12, 14, 17, 19], TIG [9, 12, 20–23], NG-TIG [12], TIG-MIG [24] and EBW [12].

Various software programmes (e.g. ABAQUS [7–9, 19, 23, 25], ANSYS [13, 15, 17, 20, 21, 26] or SYSWELD [7, 12, 22, 27]) applied in the numerical simulation of welding processes are based primarily on the Finite Element Method (FEM),

Because of many complicated calculations, the numerical simulation of the welding process requires the use of computers characterised by high computing power. The time of numerical simulation can be reduced using various simplifications. For instance, axisymmetric models or models containing 3D elements can be replaced with models containing 2D elements [7, 10, 18, 27].

The numerical simulation of the welding process should enable the obtainment of results as similar to those obtained in the actual welding process (physical simulation) as possible. However, as emphasized by the authors of works [13, 23], the foregoing necessitates taking into consideration many variables describing the heat source, welding method and its technological parameters, welding joint geometry, beading technique as well as the number and type of restraints (stiffeners). The foregoing is particularly problematic in relation to large-sized welded structures. When analysing deformations and welding strains of large-sized structures, the authors of publications [8, 19] observed the high consistence of numerical simulation results with those obtained under actual welding process conditions (physical simulation).

The authors of publication [28] presented results of numerical analyses concerning the welding of storage tanks, drawing readers' attention to the use of the Finite Element Method (FEM) in the identification of welding strains in large-sized structures. In spite of the high complexity of the welding process it is possible to perform a precise FEM-based thermo-mechanical analysis, yet its application is limited to small elements [29–32].

The modelling and calculations concerning large structures is a very time-consuming process. In order to reduce the aforesaid time it is possible to use solutions consisting in the simulation of specific welding thermal cycles in subsequent, previously selected, segments of the joint.

The study contains results of tests concerning the use of the FEM-based simulation of the welding process aimed at the minimisation of welding strains in the large-sized storage tank head (i.e. "bottom"). The numerical simulation was performed using Sysweld software (versions 15.5 and 16). The tests included analyses of various welding sequences and directions with respect to their effect on the distribution of the field of displacements at characteristic (mesh) nodes of the tank head, constituting the measure of welding strains.

2. Test material and methodology

The subject of the tests was a large-sized welded structure, i.e. the head ("bottom") of a storage tank having a diameter of 10 m. The test element was made of steel S235JR. The geometry of the storage tank head is presented in Figure 1.

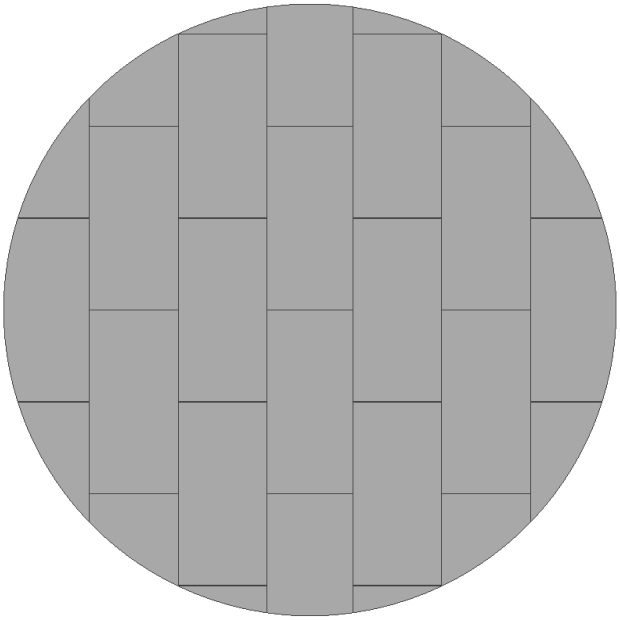

Fig. 1. Storage tank head geometry (CAD model)

The head of the tank was made of 6 mm thick plate fragments subjected (during the process) to butt and overlap welding. The making of the joints entailed the development of appropriate welding procedure specifications (WPS), enabling the performance of the process based on the MAG welding method (135).

The pre-weld preparation of elements involved the following stages:

- bevelling of the plates for butt joints (i.e. square butt weld preparation),
- positioning and tacking of the plates.

The tank head was welded in a stepped backward manner, where butt (transverse) welds were made as first and overlap (longitudinal) welds were made afterwards (Fig. 2). The welding process was performed sequentially from the centre of the tank head towards the outside. The schematic diagram below presents the making of the welds, based on the symmetric quarter of the tank head.

The scope of the tests included the development of CAD and FEM models of the mock-up of the flat element of the tank head segment as well as the subsequent performance of analyses of the FEM-based mock-ups.

The FEM-based simulation was performed for various models of welding sequence and directions. Such an approach made it possible to identify the effect of the aforesaid sequence and directions on welding distortions and strains of the storage tank head. To this end, it was necessary to modify the CAD model, composed of 3D bodies. The first stage involved the development of geometry composed of central areas, whereas the subsequent stage of the CAD model development involved the making of longitudinal and transverse welds. Butt welds were simulated using central areas, whereas overlap welds were obtained using the weld

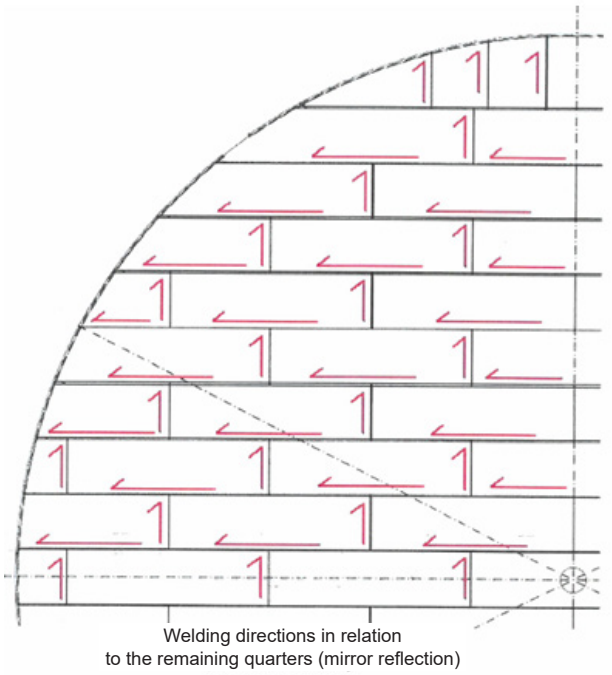

Fig. 2. Schematic diagram presenting the welding of the storage tank head

face area. The width of the butt welds was determined on the basis of weld groove geometry, in accordance with the design drawing and guidelines specified in related welding procedure specifications (WPS). The geometry was characterised by two planes of symmetry. As a result, the model and analyses involved one quarter, taking into account appropriate symmetry boundary conditions (Fig. 3). The view of the finite element mesh is presented in Figure 4.

The simulation involved the attribution of material properties of steel S235JR and thickness to individual finite elements.

The boundary conditions adopted in the tests were the following (Fig. 5):

- boundary condition 1 of symmetry in the plane perpendicular to the y-axis of the object subjected to the test,
- boundary condition 2 of symmetry in the plane perpendicular to the x-axis of the object subjected to the test,
- boundary condition 3 of restraint – lack of possibility of displacements in x-, y- and z-directions as well as the lack of the rotation around the x-, y- and z-axes of the node in the corner of the object subjected to the test.

The numerical simulation of the models concerned with welding sequence and directions included the application of the thermal shrinkage method involving the simulation of shrinkage in the area of welded joints. The value of shrinkage was defined by the thermal expansion coefficient of the material. The method involved the definition of the joint segment being welded at a given moment and the simulation of a condition triggering the shrinkage in this area.

The identification of the effect of welding sequence and directions in the numerical simulation related to the distribution of stresses and strains of the tank head involved the analysis of 4 models, where the initial model was the previously used variant of welding sequence and direction during the welding of the tank head (Fig. 6).

In the initial model, welds were made sequentially from the centre of the tank head towards the outside. Butt we-

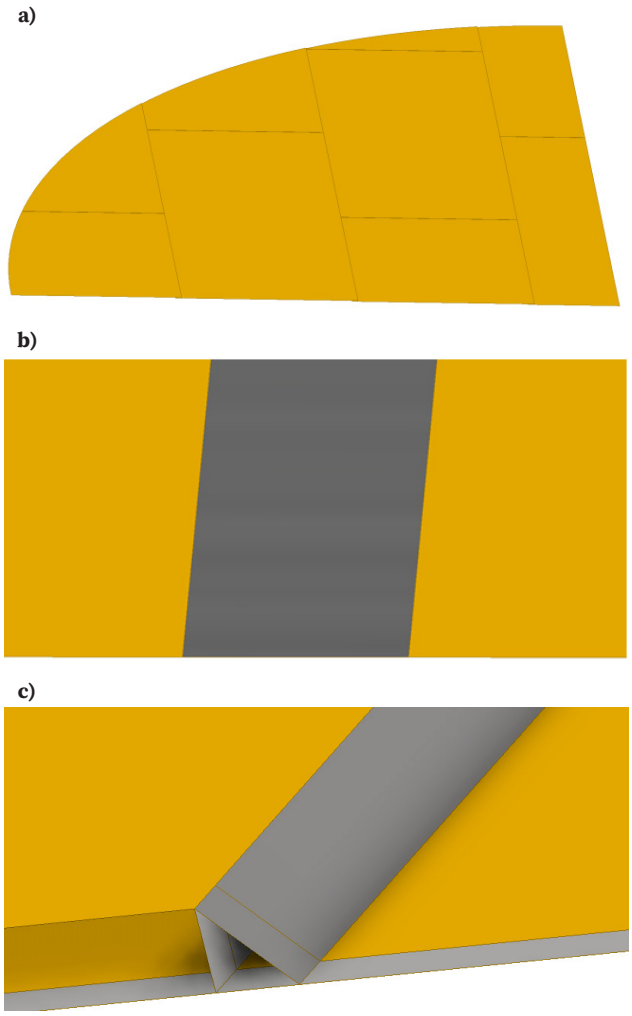

Fig. 3. Model (CAD) composed of central areas (a), butt welds simulated using central areas (b) and overlap welds simulated using the weld face area (c)

lds (designated as 1-7) were made as first, whereas overlap welds (8-11, 12-14 and 15-17) were made afterwards. In comparison with the initial model, model 2 was characterised by a change in the direction, in which overlap joints were made (i.e. from the outside to the inside). In comparison with the initial model, model 3 was characterised by a change in the sequence, in which overlap joints were made. In turn, model 4 was characterised by overlap joints made from the outside to the inside, whereas the welding direction was also defined as from the outside to the inside.

In relation to all the variants of welding sequence and directions, the forecasting of distortions was based on the analysis of the field of displacements in the x-, y- and z-directions and resultant displacements.

For the purpose of the comparative analysis of test results concerning the displacements of the tank head in the perpendicular direction, displacement values were identified in selected characteristic (mesh) nodes of the tank head, forming lines 1 and 2 (nodes 1-11, located 500 mm away from one another). The schematic diagram showing the arrangement of the nodes is presented in Figure 7.

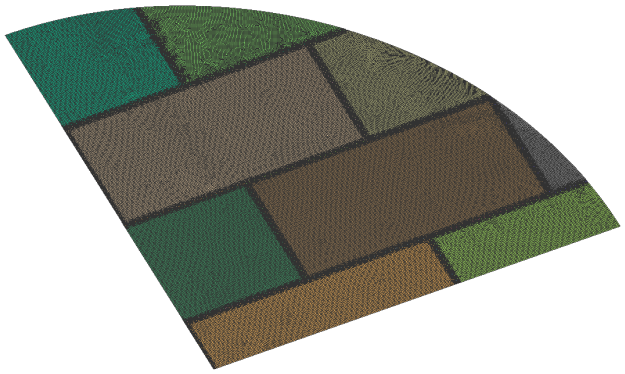

Fig. 4. Finite element mesh of the tank head model

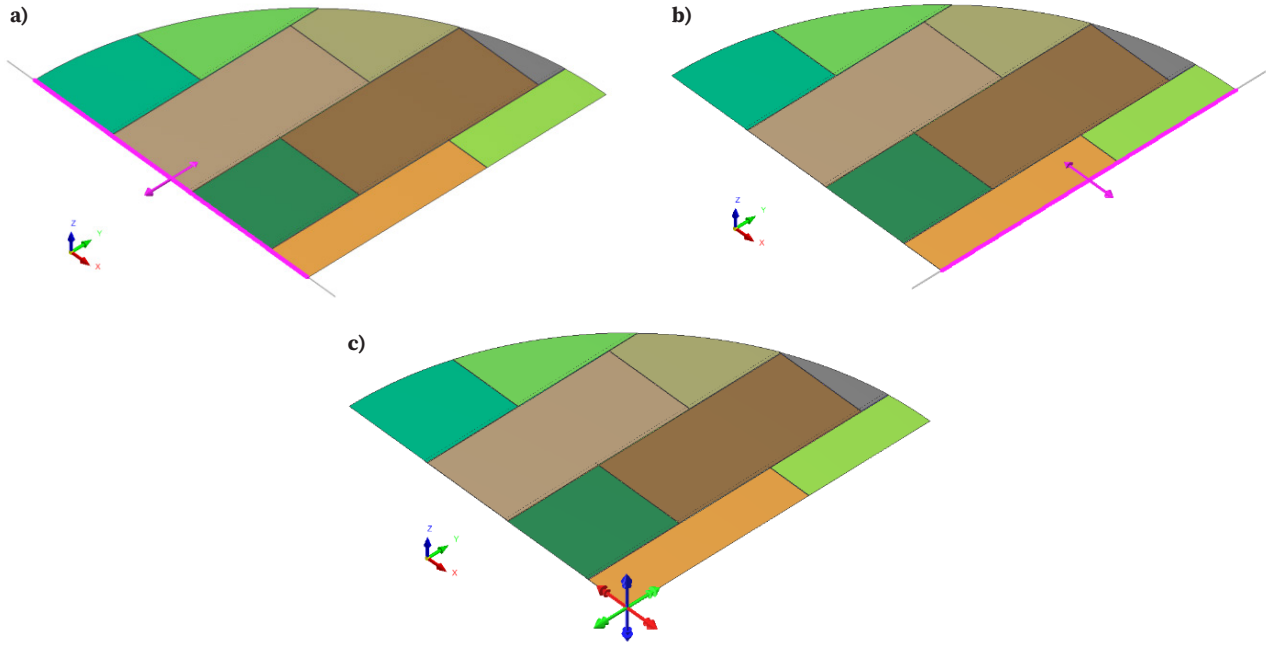

Fig. 5. Boundary conditions 1-3: a) boundary condition of symmetry in the plane perpendicular to the y-axis of the edge of the object being tested, b) boundary condition of symmetry in the plane perpendicular to the x-axis of the edge of the object being tested and c) boundary condition of restraint – lack of possibility of displacements in the x-, y- and z-directions as well as the lack of rotation around the x-, y- and z-axes of the node

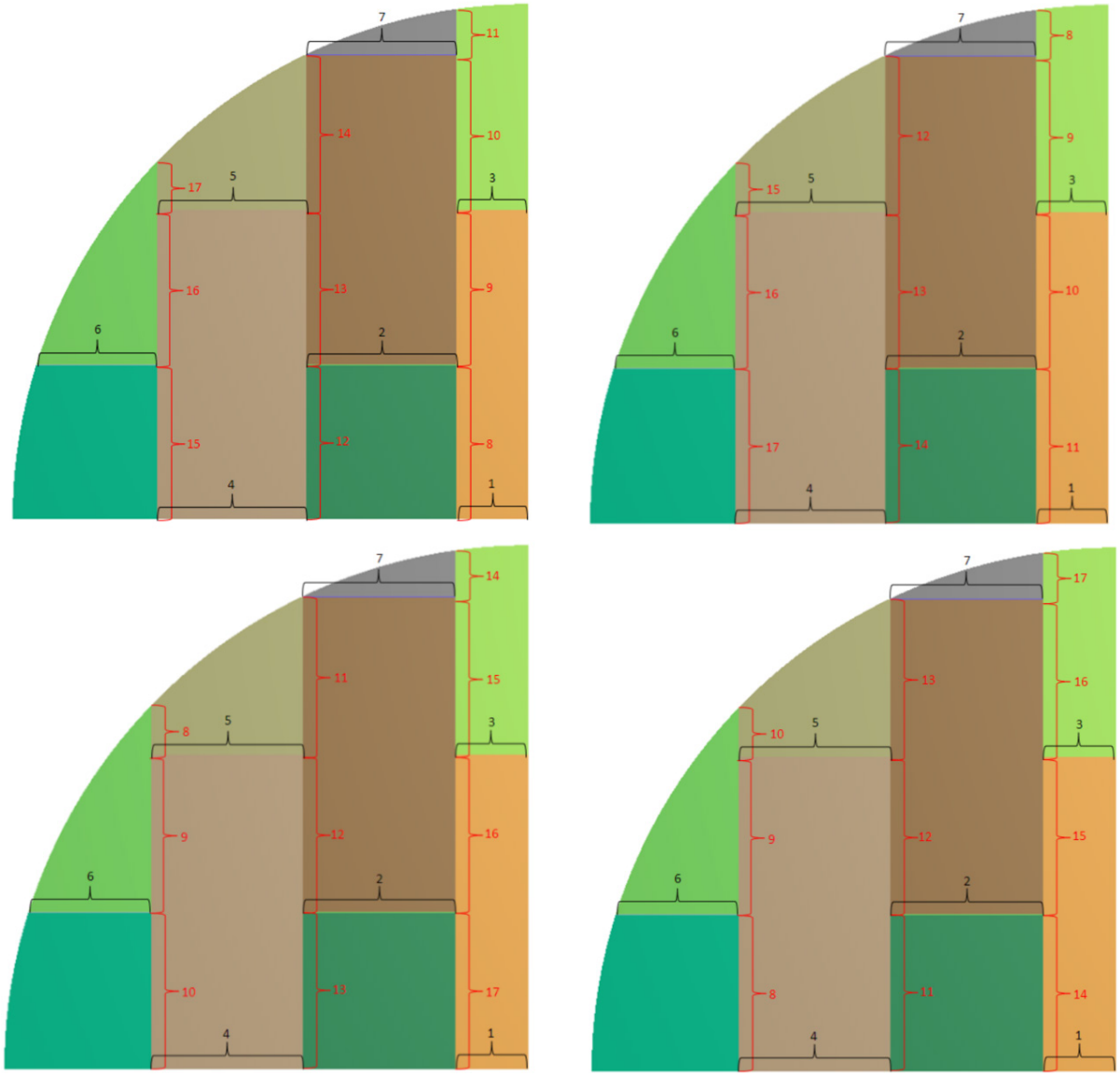

Fig. 6. Welding sequence models: a) initial model, b) model 2, c) model 3 and d) model 4

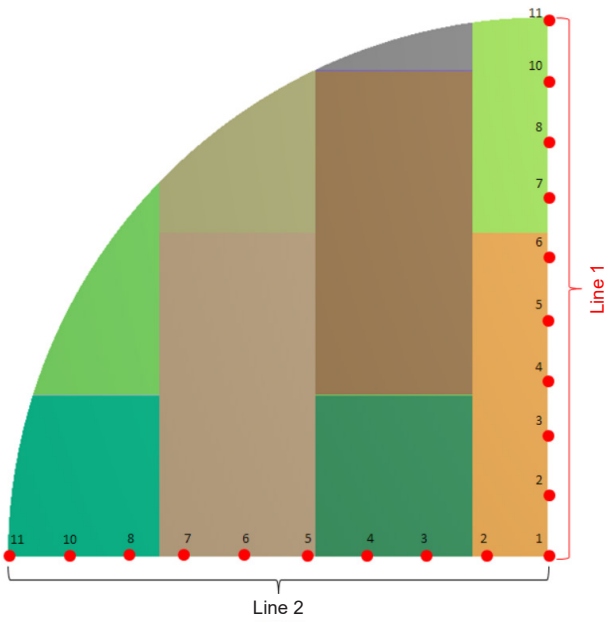

Fig. 7. Arrangement of the nodes used in the determination of displacement values /Line 1; Line 2/

3. Test results and analysis

Figures 8–10 present fields of displacements in individual directions in all the models of welding sequence and directions during the welding of the storage tank head.

The analysis of the fields of displacements in the x- and y-directions revealed similar values of displacements in all the models, with a maximum difference of not more than 0.2 mm. Table 1 contains post-weld displacements at nodes A and B (schematic diagram in Table 1) only in relation to the z-direction, i.e. where values of displacements were significant.

Figures 11 presents the field of resultant displacements in relation to the initial model and models 2-4.

The greatest displacements triggered by welding strains in the storage tank head were observed in the z-direction, i.e. perpendicular do the tank head surface. It was possible to observe surface corrugation resulting from positive and negative values of distortions, primarily resulting from the extension and compression of the material.

The greatest displacements were observed in the area of the peaks of the simulated structure, i.e. at nodes 1 and 2 (schematic diagram in Table 1). In the initial model, the lo-

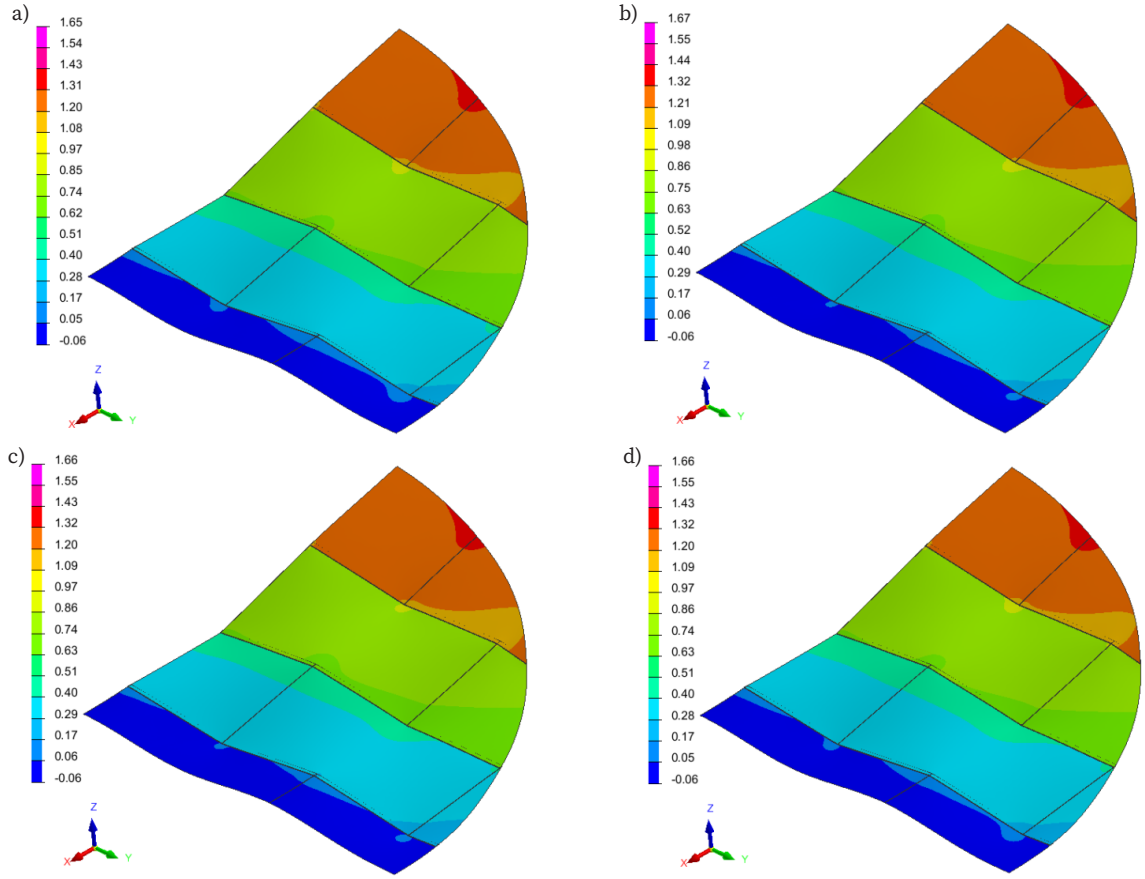

Fig. 8. Field of displacements in the x-direction: a) initial model, b) model 2, c) model 3 and d) model 4; 10-fold rescaling of element distortion, [mm]

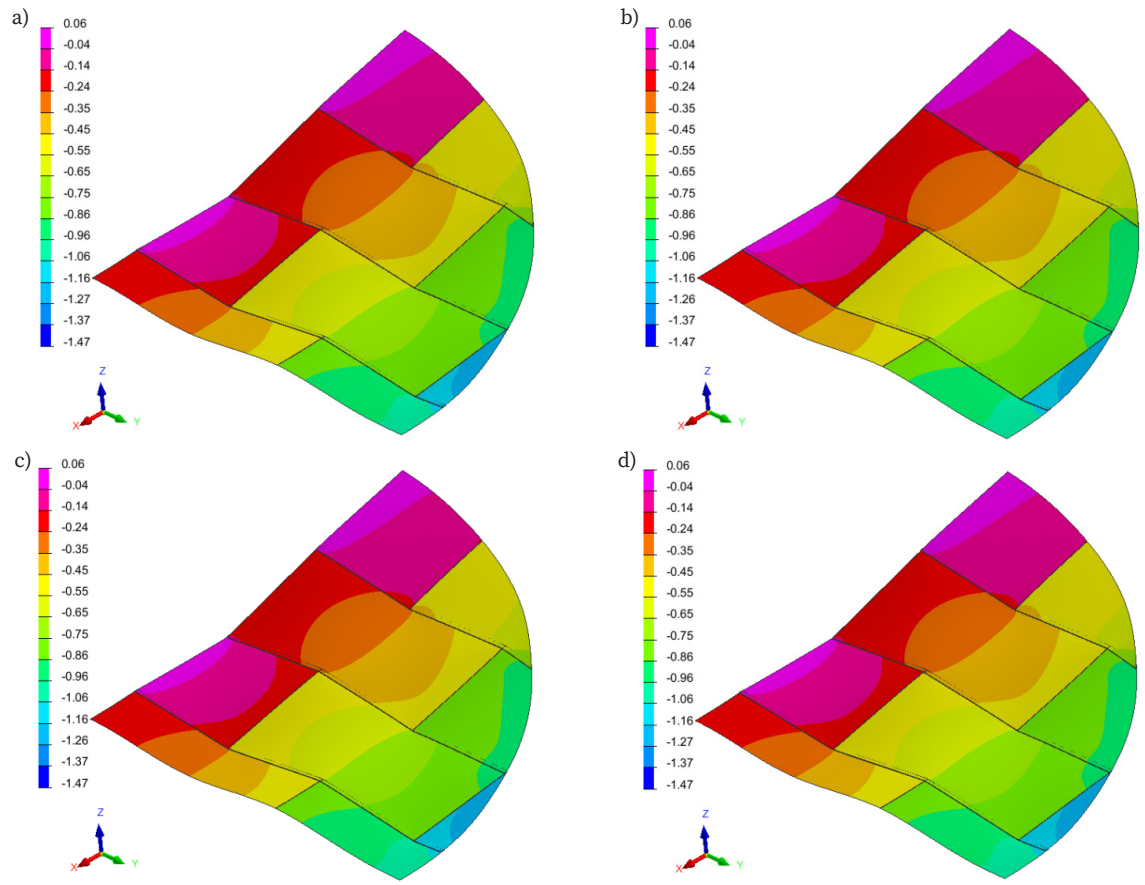

Fig. 9. Field of displacements in the y-direction: a) initial model, b) model 2, c) model 3 and d) model 4; 10-fold rescaling of element distortion, [mm]

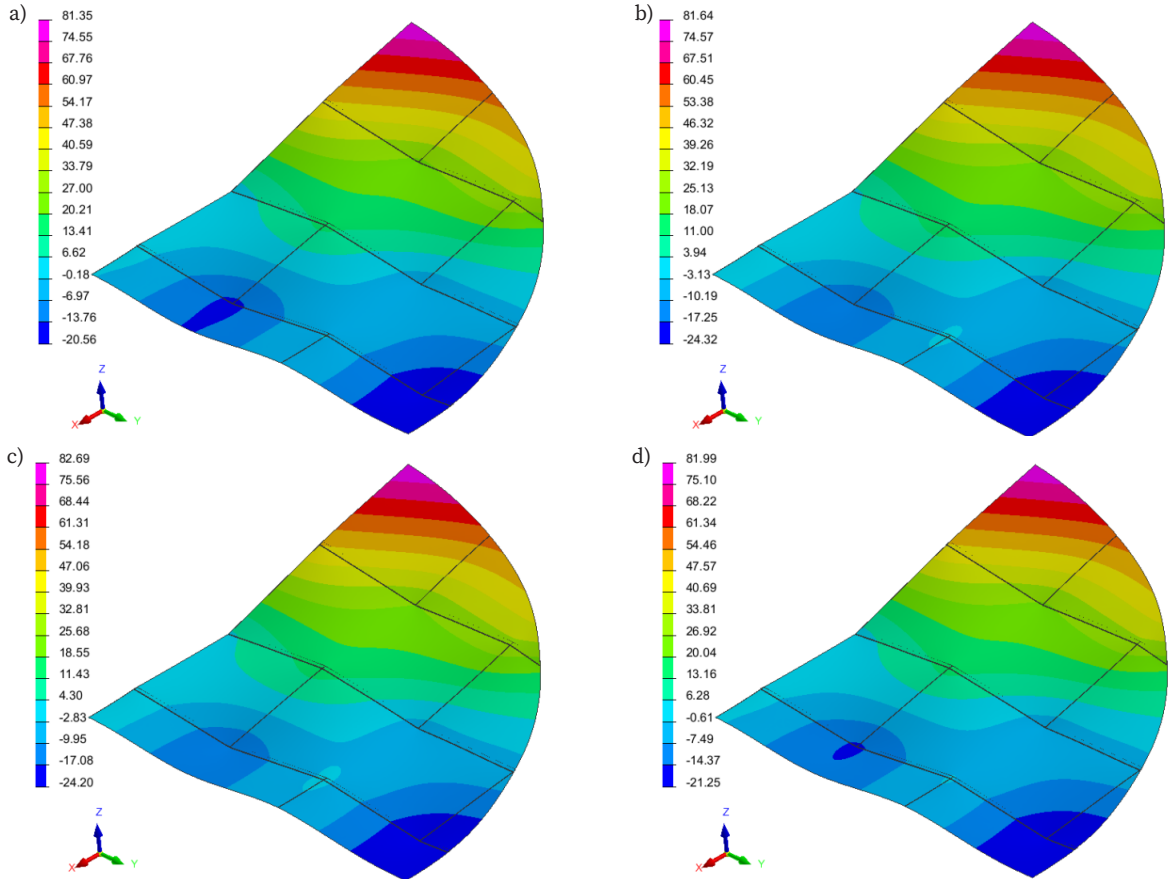

Fig. 10. Field of displacements in the z-direction: a) initial model, b) model 2, c) model 3, and d) model 4; 10-fold rescaling of element distortion, [mm]

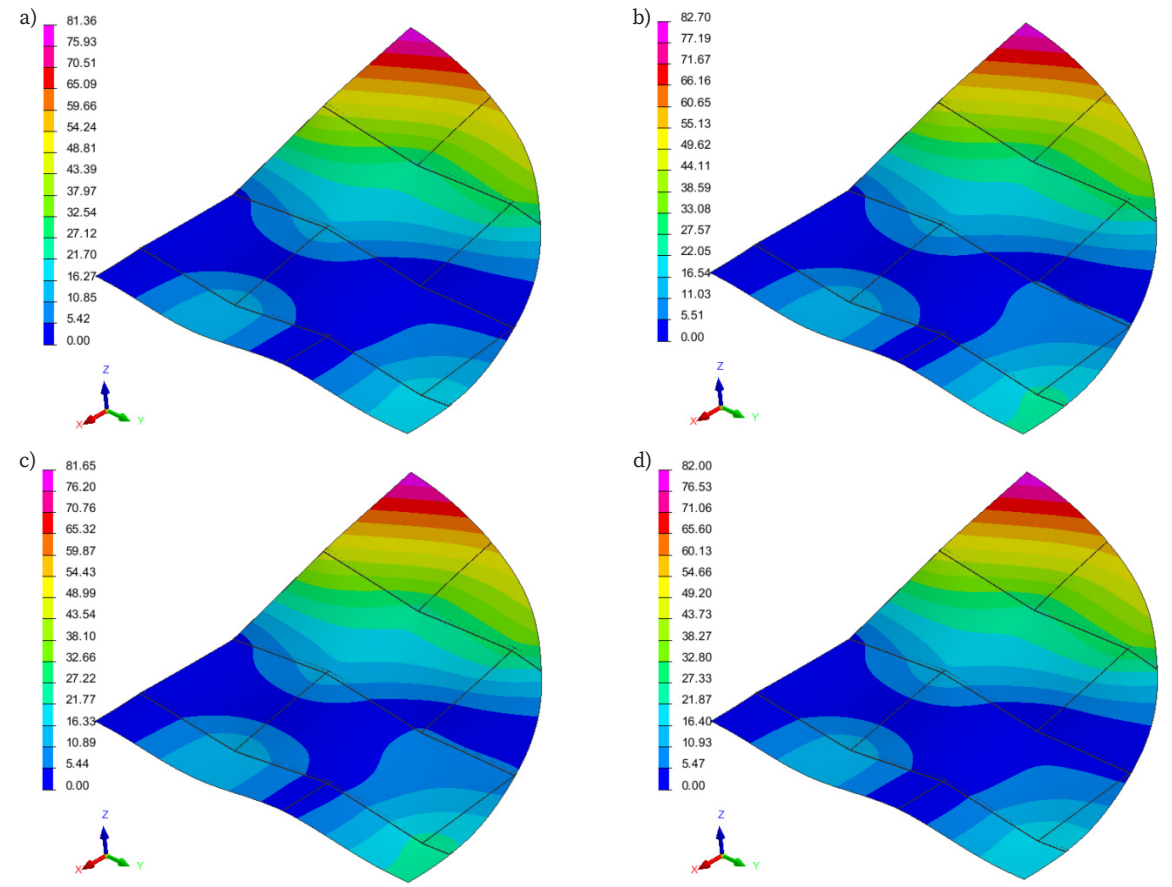

Fig. 11. Field of resultant displacements: a) initial model, b) model 2, c) model 3, and d) model 4; 10-fold rescaling of element distortion, [mm]

Table 1. Displacement after welding in the z-direction /Node A; Node B/

Initial model	Displacement in z-direction, [mm]		Difference in displacements between nodes 1 and 2, [mm]	Difference in displacements in relation to the initial model, [%]	
	Node A	Node B		Nodet A	Node B
	-17.95	81.35	99.30	-	-
2	-22.78	82.69	105.47	21.20	1.62
3	-22.84	81.64	104.48	21.41	0.36
4	-18.92	81.99	100.91	5.13	0.78

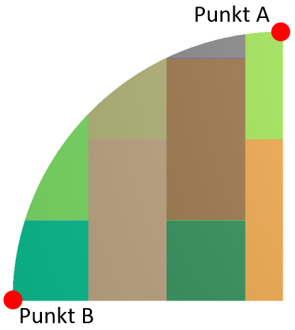

west values of displacements were observed at mesh nodes A and B. At mesh node A, the difference between the initial model and models 2-4 amounted to 21.20 %, 21.41 % and 5.13 % respectively. At node B, the difference between the initial model and models 2-4 amounted to 1.62 %, 0.36 % and 0.78 % respectively.

Values of displacements in the z-direction at mesh nodes on measurement lines 1 and 2 (Fig. 7) are presented in Figures 12–15.

The results obtained in the tests revealed significant differences in values of displacements at individual mesh nodes on lines 1 and 2 in all the welding sequence and direction-related models.

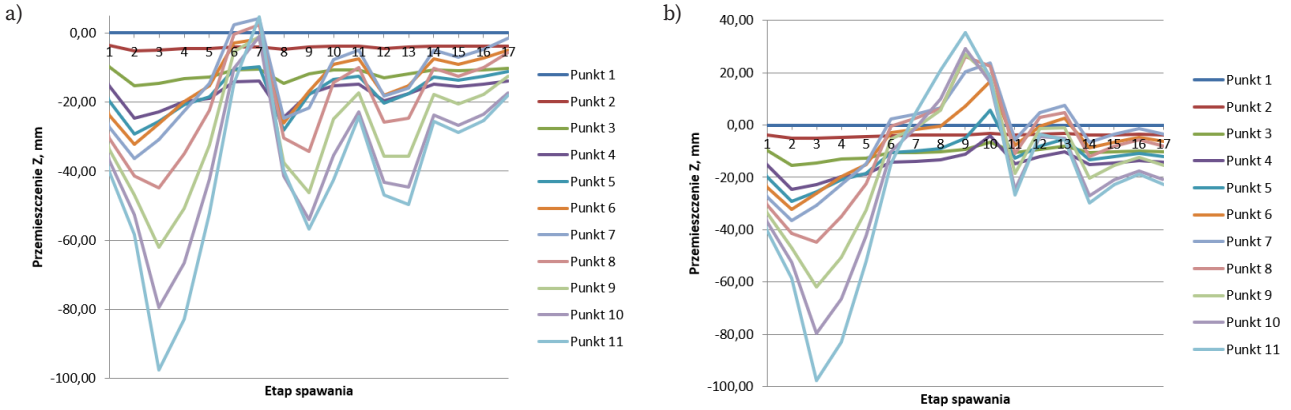

Fig. 12. Results of displacements in the z-direction at selected mesh nodes on line no. 1 at successive welding stages: a) initial model and b) model 2 /Displacement; Welding stage; Node/

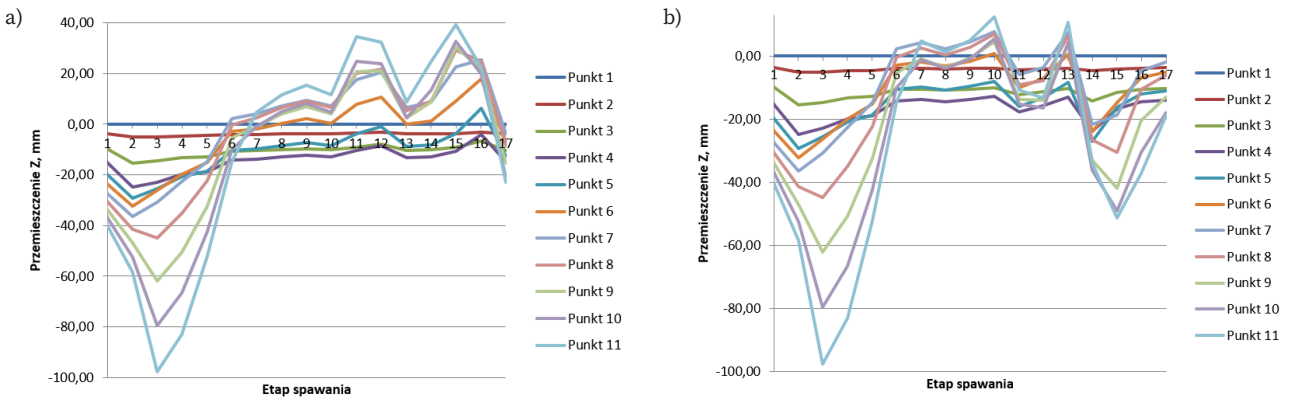

Fig.13. Results of displacements in the z-direction at selected mesh nodes on line no. 1 at successive welding stages: a) model 3 and b) model 4 /Displacement; Welding stage; Node/

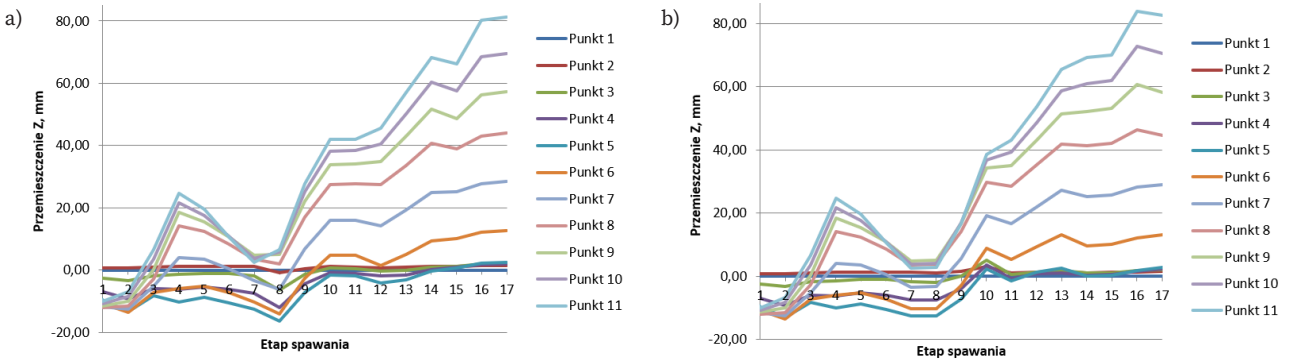

Fig. 14. Results of displacements in the z-direction at selected mesh nodes on line no. 2 at successive welding stages: a) initial model and b) model 2 /Displacement; Welding stage; Node/

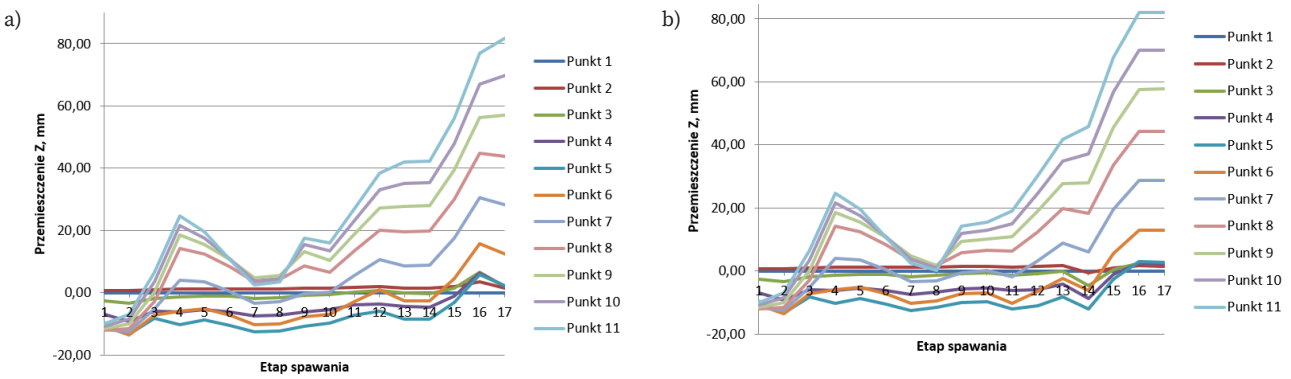

Fig. 15. Results of displacements in the z-direction at selected mesh nodes on line no. 2 at successive welding stages: a) model 3 and b) model 4

The analysis of displacements during individual stages of the welding of the tank head (i.e. stages 1-17) revealed that at the first seven stages, connected with the making of butt (transverse) welded joints, there were no differences observed between the models. The above-presented situation resulted from the lack of differences as regards welding sequence in relation to all the models subjected to analysis.

At stages involving the making of overlap (longitudinal) joints, which in the initial model and in models 2-4 were welded in differences sequences, it was possible to observe differences in values and (-z- and +z) directions of displacements.

In terms of line 1 (Fig. 12) of the initial model it was observed that most displacements at stages 8-17 were in the z-direction. The minimum value amounted to -56.66 mm. In model 2, displacements at stages 8-17, observed in the +z- and –z-directions, were restricted within the range of -29.75 mm to 35.33 mm. In model 3, at stages 8-17, most displacements were observed in the +z-direction; the maximum value amounting to 39.25 mm. In model 4, at stages 8-17, displacements were observed in the +z- and –z-directions; the values of displacements were restricted within the range of -51.11 mm to 12.32 mm.

As regards line 2 (Fig. 13), displacements at stages 8-17, along with successive welding stages, increased in the +z--direction. It was also possible to observe differences as regards the increase in the aforesaid differences. Significant differences were observed in welding areas at stages 8-16. In the last joint (i.e. stage 17), displacement-related results were similar in relation to all of the models.

The first seven stages were not characterised by differences between the models; most of the displacements on line 1 were in the –z-direction.

On line 1, at welding stages 8, 9 and 10 and at mesh nodes 1-5, the tank head was characterised by displacements in the –z-direction, with the highest absolute values observed in the initial model. At mesh nodes 7-11 it was possible to observe a change in the direction of displacements from –z to +z. In all the models it was possible to observe that the absolute values of displacements increased. At stage 11 of the welding process it was possible to observe a change in the direction of displacements in models 2 and 4. Stage 12 was characterised by a significant decrease in the absolute value of displacements in models 2 and 4. In turn, stage 13 was characterised by decreased displacements visible in model 3. At stages 14-16, in models 2 and 4, mesh nodes 7-11 were displaced in the –z-direction. After the completion of the welding process (stage 17), all the nodes in the models were characterised by similar displacements in the –z-direction, obtaining the highest value at mesh node 11.

On line 2, the first seven stages were not characterised by differences between the models; displacements were both in the –z and +z-directions. At stages 1 and 2, most of the mesh nodes were displaced in the –z-direction. At stage 3 it was possible to observe a change in the direction of displacements, where at mesh nodes 3-8, the displacements were observed in the –z-direction. Stage 4 at mesh nodes 7 and 8 was characterised by a change in the direction of displacements (+z-direction). It was also possible to notice an increase in the absolute value of displacement from a maximum of 8.20 mm (stage 3 of the welding process) to 24.71 mm (stage 4 of the welding process). In turn, stages 5-7 were characterised by a decrease in absolute values of displacements.

At stage 8 (the initiation of the welding of overlap joints) it was possible to notice differences between numerical

calculation results in relation to the models subjected to analysis. At stage 9, the greatest displacements were characteristic of the initial model, whereas the displacement-related tendency along the length of line 2 remained unchanged. Stage 10 was characterised by decreased values of displacements in the –z-direction at mesh nodes 4-6 and by increased values of displacements in the +z-direction at mesh nodes 7-11 in the initial model and in model 2. Stages 11-14 were characterised by a further increase in displacements at nodes 7-11 in all the models. The greatest absolute displacements in the +z-direction were observed in relation to model 2. At stage 15 of the welding process, in all the models it was possible to observe similar values and nature of displacements at nodes 1-11. Stages 16 and 17 were characterised by a further increase in displacements and, at the same time, an increase in the convergence of results in relation to individual models.

The numerical simulation results revealed that, during welding, the initial model could be characterised by greater displacements in relation to those observed in models 2-4. As regards line 1, higher values were observed at stages 8-10, 12 and 13. In turn, in terms of line 2, higher values were observed at stages 8-10. On line 2, at stages 11-14, it was possible to observe greater displacements in the initial model than those observed in models 3 and 4.

The calculation results following the completion of the welding process (stage 17) are presented in Table 2. In addition, Table 2 presents differences concerning the displacements in models 2-4 in relation to those of the initial model (marked red).

The results obtained in the calculations revealed that in terms of line l and nodes 2-11, the displacements in the initial model were smaller than those observed in models 3 and 4. In turn, the displacements at mesh nodes 3-11 in model 2 where greater than those observed in the initial model.

In relation to line 2 and mesh nodes 2-11 it was possible to observe that the displacements in the initial model were smaller only in relation to those observed in model 4. In model 2 at mesh nodes 3-11 on line 2 the displacements were greater in comparison with those observed in the initial model. In model 3 at nodes 10 and 11 it was possible to observe greater displacements than those observed in the initial model. In turn, the displacements observed at mesh nodes 2-9 of the initial model were greater.

4. Concluding remarks

The above-presented numerical test results justified the formulation of the following conclusions:

- The use of varied welding sequences and directions during the welding of the storage tank head resulted in the obtainment of various values in the distribution of the field of displacements (distortions). After the completion of the welding process in the initial model and models 2-4, the distributions of the field of displacements were characterised by different displacement-related values and the similar nature of tank head corrugations triggered by welding strains.
- Dimensionally relevant displacements (distortions) of the storage tank head were observed in the z-direction (perpendicular to the head surface). In all the models of welding sequences and directions, the greatest displacements were observed in the area of the peaks of the tank head quarter subjected to analysis.
- In relation to the initial model (i.e. the variant used previously during the welding of the tank head) the analysis revealed that the remaining models 2-4 at mesh node A were characterised by displacements greater by a maximum of 5.13% (model 4), 21.41% (model 3) and 21.20%

Table 2. Values of post-weld displacements and differences in the displacements observed in models 2-4 in relation to the initial model (marked grey)

Line 1

		Node 1	Node 2	Node 3	Node 4	Node 5	Node 6	Node 7	Node 8	Node 9	Node 10	Node 11
Initial model		0.00	-3.71	-10.26	-13.96	-11.03	-5.03	-1.60	-5.70	-12.41	-17.25	-17.95
Model 2		0.00	-3.70	-10.29	-14.32	-11.91	-6.36	-3.51	-8.14	-15.31	-20.97	-22.78
Model 3		0.00	-3.72	-10.39	-14.63	-12.43	-6.89	-3.92	-8.37	-15.44	-21.05	-22.84
Model 4		0.00	-3.73	-10.30	-14.00	-11.07	-5.12	-1.81	-6.07	-12.98	-18.01	-18.92
Difference in displacements in relation to the initial model [%]	Model 2	-	-0.27	0.29	2.51	7.39	20.91	54.42	29.98	18.94	17.74	21.20
	Model 3	-	0.27	1.25	4.58	11.26	27.00	59.18	31.90	19.62	18.05	21.41
	Model 4	-	0.54	0.39	0.29	0.36	1.76	11.60	6.10	4.39	4.22	5.13

Line 2

		Node 1	Node 2	Node 3	Node 4	Node 5	Node 6	Node 7	Node 8	Node 9	Node 10	Node 11
Initial model		0.00	1.52	2.10	2.06	2.48	12.69	28.42	44.01	57.21	69.53	81.35
Model 2		0.00	1.49	2.15	2.29	2.77	13.08	28.90	44.57	58.08	70.65	82.69
Model 3		0.00	1.41	1.93	1.91	2.28	12.43	28.13	43.71	57.14	69.66	81.64
Model 4		0.00	1.53	2.22	2.28	2.76	13.04	28.79	44.41	57.69	70.09	81.99
Difference in displacements in relation to the initial model [%]	Model 2	-	-2.01	2.33	10.04	10.47	2.98	1.66	1.26	1.50	1.59	1.62
	Model 3	-	-7.80	-8.81	-7.85	-8.77	-2.09	-1.03	-0.69	-0.12	0.19	0.36
	Model 4	-	0.65	5.41	9.65	10.14	2.68	1.29	0.90	0.83	0.80	0.78

(model 2) respectively. At node B, the models were characterised by displacement greater by 0.78% (model 4.), 0.36% (model 3) and 1.62% (model 2) respectively. At the same time, the results concerning displacements along lines 1 and 2 indicated that selected mesh nodes of the initial model were characterised by higher values of displacements than those observed in models 2 and 3.

- At the first seven stages, involving the making of butt welded joints, no differences in the distribution of the field of displacements were observed. The foregoing resulted from the lack of differences in welding sequence (in all the models). The stages involving the making of overlap joints, which, in the initial model and models 2-4 were made using different sequences, revealed differences in both values and directions (-z and +z) of displacements along the lines subjected to analysis.
- Selected welding stages of the initial model were characterised by greater displacements than those observed in models 2-4. In relation to line 1, greater values were observed at stages 8-10, 12 and 13. I turn, as regards line 2, greater displacements were observed at stages 8-10. In relation to line 2 and stages 11-14 it was possible to observe greater displacements in the initial model than those observed in models 3 and 4. The above-presented situation necessitates the performance of further analyses aimed to reduce the formation of strains during subsequent welding stages.
- The FEM-based analysis of the storage tank head mock-up enabled the qualitative verification of the scheme concerning the welding of the tank in terms of welding strains. As regards the models subjected to analyses, the reduction of welding strains requires the performance of additional analyses, taking into account, among other things, other methods enabling the reduction of strains (e.g. a system of restraints).

Acknowledgements

The project was co-financed by the European Union from the European Regional Development Fund within the Regional Operational Programme for the Podlaskie Voivodeship in the years 2014-2020 within Measure 1.2 Industrial Research and Development Work and Their Implementation. Project type: R&D works. Project title: The Numerical Analysis Results-Based Development of an Innovative Technology of the Prefabrication of Welded Structures, Pipelines and Elements of Pressure Equipment.

REFERENCES

[1] Pilarczyk J. [red.] at all: Poradnik inżyniera. Spawalnictwo, cz. 1. Wydawnictwa Naukowo-Techniczne, Warszawa 2021.
[2] Pilarczyk J., Pilarczyk J.: Spawanie i napawanie elektryczne metali. Wyd. Śląsk, Katowice 1996.
[3] Pikuła J., Pfeifer T., Mendakiewicz J.: Influence of the shielding gas on the properties of VP MIG/MAG braze-welded joints in zinc coated steel sheets. Biuletyn Instytutu Spawalnictwa w Gliwicach, 2014, vol. 58, no. 1, pp. 35-41.
[4] Kiszka A., Pfeifer T.: Spawanie cienkich blach stalowych z powłokami ochronnymi metodą MAG prądem o zmiennej biegunowości. Biuletyn Instytutu Spawalnictwa w Gliwicach, vol. 56, no. 2, 2012, pp. 39-43.
[5] Gawrysiuk W., Pfeifer T., Winiowski A.: Charakterystyka technologii lutospawania łukowego MIG/MAG. Przegląd Spawalnictwa, 2005, no. 2-3, pp. 17.
[6] Bruckner J.: Metoda CMT – rewolucja w technologii spawania. Przegląd Spawalnictwa, 2009, no. 7-8, pp. 24.
[7] Lee S.H., Kim E.S., Park J.Y., Choi J.: Numerical analysis of thermal deformation and residual stress in automotive muffler by MIG welding. Journal of Computational Design and Engineering, 2018, vol. 5, pp. 382-390.
[8] Perić M., Seleš K., Tonković Z., Lovrenić-Jugović M.: Numerical simulation of welding distortions in large structures with a simplified engineering approach. Open Physics, 2019, vol. 17, pp. 719-730.
[9] Domański T., Piekarska W., Saternus Z., Kubiak M., Stano S.: Numerical Prediction of Strength of Socket Welded Pipes Taking into Account Computer Simulated Welding Stresses and Deformations. Materials, 2022, vol. 15, 3243.
[10] Islam M., Buijk A., Rais-Rohani M., Motoyama K.: Simulation-based numerical optimization of arc welding process for reduced distortion in welded structures. Finite Elements in Analysis and Design, 2014, vol. 84, pp. 54-64.
[11] Potukutchi R., Agrawal H., Perumalswami P.: Fatigue Analysis of Steel MIG Welds in Automotive Structures. SAE Technical Paper Series. 2004 SAE World Congress, Detroit, Michigan, March 8-11, 2004.
[12] Prakash R., Gangradey R.: Review of high thickness welding analysis using SYSWELD for a fusion grade reactor. Fusion engineering and Design, 2013, vol. 88, pp. 2581-2584.
[13] Farias R.M., Teixeira P.R.F., Araújo D.B.: Thermo-mechanical analysis of the MIG/MAG multi-pass welding process on AISI 304L stainless steel plates. Journal of the Brazilian Society of Mechanical Sciences and Engineering, 2017, vol. 39, pp. 1245-1258.
[14] Ogino Y., Hirata Y., Murphy A.B.: Numerical simulation of GMAW process using Ar and an Ar–CO_2 gas mixture. Weld World, 2016, vol. 60, pp. 345-353.
[15] Zhu W., Xu Ch., Zeng L.: Coupled finite element analysis of MIG welding assembly on auto-body high-strength steel panel and door hinge. The International Journal of Advanced Manufacturing Technology, 2010, vol. 51, pp. 551-559.
[16] Sakri A., Guidara M., Elhalouani F.: Numerical simulation of MIG type arc welding induced residual stresses and distortions in the sheets of S235 steel. Materials Science and Engineering, 2010, vol. 13, 012020.
[17] Barsoum Z., Lundbäck A.: Simplified FE welding simulation of fillet welds – 3D effects on the formation residual stresses. Engineering Failure Analysis, 2009, vol. 16, pp. 2281-2289.
[18] Li W., Yu R., Huang D., Wu J., Wang Y., Hu T., Wang J.: Numerical simulation of multi-layer rotating arc narrow gap MAG welding for medium steel plate. Journal of Manufacturing Processes, 2019, vol. 45, pp. 460-471.
[19] Perić M., Tonković Z., Rodić A., Surjak M., Garašić I., Boras I., Švaić S.: Numerical analysis and experimental investigation of welding residual stresses and distortions in a T-joint fillet weld. Materials and Design, 2014, vol. 53, pp. 1052-1063.
[20] Vemanaboina H., Akella S., Buddu R.K.: Welding process simulation model for temperature and residual stress analysis. Procedia Materials Science, 2014, vol. 6, pp. 1539-1546.
[21] Varma Prasad V.M., Joy Varghese V.M., Suresh M.R., Siva Kumar D.: 3D simulation of residual stress developed during TIG welding of stainless-steel pipes. Procedia Technology, 2016, vol. 24, pp. 364-371.
[22] Koňár R., Patek M.: Numerical simulation of dissimilar weld joint in Sysweld simulation software. Tehnički vjesnik, 2017, vol. 24, Suppl. 1, pp. 137-142.
[23] Deng D.: FEM prediction of welding residual stress and distortion in carbon steel considering phase transformation effects. Materials and Design, 2009, vol. 30, pp. 359-366.
[24] Han Y., Chen J., Ma H., Zhao X., Wu Ch., Gao J.: Numerical simulation of arc and droplet behaviors in TIG-MIG hybrid Welding. Materials, 2020, vol. 13, 4520.
[25] Finch D.M., Burdekin F.M.: Effects of welding residual stresses on significance of defects in various types of welded joint. Engineering Fracture Mechanics, 1992, vol. 41, no. 5, pp. 721-735.
[26] Barsoum Z., Barsoum I.: Residual stress effects on fatigue life of welded structures using LEFM. Engineering Failure Analysis, 2009, vol. 16, pp. 449-467.

[27] Giętka T., Ciechacki K., Kik T.: Numerical simulation of duplex steel multipass welding. Archives of Metallurgy and Materials, 2016, vol. 61, no. 4, pp. 1975-1984.
[28] Hübner A., Teng, J. G., Saal, H.: Buckling behaviour of large steel cylinders with patterned welds. International Journal of Pressure Vessels and Piping, 2006, vol. 83, pp. 13-26.
[29] Heinze C., Schwenk C., Rethmeier M.: The effect of tack welding on numerically calculated welding-induced distortion. Journal of Materials Processing Technology, 2012, vol. 212, pp. 308-14.
[30] Li Y., Wang K., Jin Y., Xu M., Lu H.: Prediction of welding deformation in stiffened structure by introducing thermo-mechanical interface element. Journal of Materials Processing Technology, 2015, vol. 216, pp. 440-446.
[31] Fu G., Lourenço M.I., Duan M., Estefen S.F.: Influence of the welding sequence on residual stress and distortion of fillet welded structures. Marine Structures, 2016, vol. 46, pp. 30-55.
[32] Zhou Q., Wang, Y., Choi S.-K., Cao L., Gao Z.: Robust optimization for reducing welding-induced angular distortion in fiber laser keyhole welding under process parameter uncertainty. Applied Thermal Engineering, 2018, vol. 129, pp. 893-906.